A Modified Version of L-PICOLA to Output the Gravitational Potential

Philipp Miotti*, Raphael Sgier†

Institute for Particle Physics and Astrophysics, Department of Physics,
ETH Zurich, Wolfgang-Pauli-Strasse 27, 8093 Zurich, Switzerland

February 7, 2018

Abstract

We modified the N-body simulation code L-PICOLA to output the gravitational potential at particle's positions and on a mesh in – both snapshot mode – calculated in its Particle-Mesh algorithm. After solving the gravitational poisson equation of dark matter particles in a comoving frame, we found that the output of our pipeline is consistent with its mass overdensity. The spherical harmonic power spectrum of the potential shows an agreement within 10 % at scales $l \lesssim 30$ and $l \gtrsim 100$, and around ~ 15 % for $30 \lesssim l \lesssim 100$. The averages of the potential over concentric shells from the centre of the simulation box as a function of its radius differ no more than 10 % in all shells. From the probability density function of the outputs we found, that the difference of the means is less than 3.3 % relatively to the RMS of their standard deviation. Our modifications can be useful to construct lensing-potential and deflection-angle maps from a fast and accurate alternative to other other N-body simulations, such as GADGET-2.

Contents

*miottiph@student.ethz.ch
†rsgier@phys.ethz.ch

1 Introduction

Recent cosmological models suggest that the formation of very large structures in the universe is based on the gravitational amplification of small density perturbations. This large-scale clustering can be calculated only partly in the linear regime at the smallest scales. The only tools to describe the structure formation on very small scales in the non-linear regime with a high accuracy to compete with present cosmological surveys are N-Body simulations. A simulations which meets these great demands in accuracy and performance is GADGET-2 [1]. On the other a large sample of simulations is necessary to increase the statistical significance of cosmological surveys. The new generation of parallelized N-body simulations, like L-PICOLA [2], provide a balance between these two needs.

The goal of this paper is to introduce modifications of L-PICOLA to compute and output of the gravitational potential at particle's position as well as on a 3-dimensional mesh in snapshot mode. It is a computational feature which is present in GADGET-2, but lacks in L-PICOLA yet. Knowing the gravitational potential of an simulation output is a great advantage to construct all-sky weak-lensing-potential and deflection-angle maps and to reduce the statistical noise in the covariance matrix, which is clearly limited by the computational power [3]. It was found that the power spectra of approximate dark matter fields from L-PICOLA agree with that from GADGET-2 to within 5 % on all scales of interest to Baryon Acoustic Oscillation [4] and Redshift Space Distortions [5] measurements, and to within 20 % up to $k = 1.0\,h\,\mathrm{Mpc}^{-1}$ [2]. In therms speed is L-PICOLA able to produce a dark matter simulation 3 orders of magnitude faster than the fully non-linear N-body simulation GADGTE-2 [2].

This paper is organized as follows. In section 2 we briefly introduce the poisson equation relating the gravitational potential with the mass overdensity and introduce dimensionless variables for our calculations. We discuss in details about the modifications of L-PICOLA we made to output the gravitational potential at particle's position and on the mesh in section 3. Section 4 provides a description of a test simulation and tools we used to verify the output of our modified code. We perform a statistical analysis in section 5 of the potential by computing the spherical harmonic power spectrum, the average as a function of distance from the centre of the simulation box and the probability distribution function. Lastly, the results are discussed in section 6.

2 Model equations and dimensionless variables

In this section we present the dimensionless poisson equation of the gravitational potential ϕ of dark matter particles (DM) for periodic boundary conditions in a comoving reference frame. This equation is solved in the Particle-Mesh (PM) algorithm of L-PICOLA [2]. For a good review and implementation of this method see [6] and [7].

The dynamics of a system of DM in a computational box of size L^3 is governed by

$$\nabla^2\phi(\mathbf{x}) = 4\pi G\Omega_{m,0}\rho_{cr,0}\delta(\mathbf{x})a^{-1}, \quad \rho_{cr,0} = \frac{3H_0^2}{8\pi G}, \quad \delta(\mathbf{x}) \equiv \frac{\rho(\mathbf{x}) - \bar{\rho}}{\bar{\rho}}, \tag{1}$$

where $\Omega_{m,0}$ is the matter density parameter, $\rho_{cr,0}$ is the critical density and δ is the overdensity with respect to the $\Omega_{m,0}$ fraction of $\rho_{cr,0}$ at a specific time $a(t) = (1+z)^{-1}$. All cosmological parameters with a subscript $'0'$ refer to the present value ($z = 0$). To solve the discrete version

of Eq. (1) on a equidistant mesh, we introduce the length of a cell x_0 and the unit of time $1/H_0$ with the Hubble constant $H_0 = 100\,h\,\mathrm{km\,s^{-1}\,Mpc^{-1}}$. Now, we can cast Eq. (1) into the following dimensionless form (tildes will denote dimensionless variables - code units):

$$\tilde{\nabla}^2\tilde{\phi}(\tilde{\mathbf{x}}) = \frac{3}{2}\frac{\Omega_{m,0}}{a}\left(\tilde{\rho}(\tilde{\mathbf{x}}) - 1\right), \tag{2}$$

where we used the variable transformations:

$$\mathbf{x} = x_0\tilde{\mathbf{x}}, \quad t = \tilde{t}/H_0, \tag{3}$$

$$\phi = \tilde{\phi}\left(x_0 H_0\right)^2, \quad \rho = \tilde{\rho}\frac{3H_0^2}{8\pi G}\frac{\Omega_{m,0}}{a^3}. \tag{4}$$

Now, we approximate $\tilde{\rho}$ on a discrete mesh. Let N_{mesh} and N_{sample} be the number of mesh cells and the number of particles respectively in one direction, and N the total number of particles in one cell. The density in a single cell of the box can be written as $\rho_{i,j,k} = M/L^3$, where $i, j, k = 1, ..., N_{mesh}$ and M is the total mass inside the cell. By virtue of Eq. (4) and the particle's mass $m = \Omega_{m,0}\rho_{cr,0}\left(L/N_{sample}\right)^3$ we get $\tilde{\rho}_{i,j,k} = N\left(N_{mesh}a/N_{sample}\right)^3$. In L-PICOLA this is done by the Cloud-in-Cell (CIC) assignment at each mesh node [2].

From this point we can solve Eq. (2) for $\tilde{\phi}$ with two methods using the discrete Fourier transform (DFT). In section 3 we will transform the equation to Fourier space from the start and then apply the discretization. The Laplace operator then converts to merely a factor $-\mathbf{k}^2$. In section 5 however, we will first write the Laplace operator in discrete form and the and solve the equation in Fourier space.

3 Modifications of L-PICOLA

With the introduction of dimensionless equations and variables in the previous section, we are now prepared to present the modifications of L-PICOLA to output the gravitational potential at particle's position and on the mesh for snapshot simulations. First, we created a new data member of the particle and wrote the potential from the initial conditions in `2LPT.c` to a new variable. In `auxPM.c` we copied the value of the potential $\tilde{\phi}$ from an intermediate step of the PM algorithm. Finally, we added this new data member to the output files in both ASCII format and unformatted binary. Like all other variables in the source file, we defined new variables in `vars.c` and `vars.h`, an new. In order to compile the modified code with the option to output the potential at the particle's position, the preprocessor directive `POTENTIAL` needs to be defined in the `Makefile`. If the potential on the mesh is requested, the directive `GONGRID` must be enabled additionally. All modifications refer to L-PICOLA v1.2, December 2015[1].

The calculation of $\tilde{\phi}$ in L-PICOLA first appears in generating the initial conditions of the particles using second order Lagrangian perturbation theory (2LPT) utilized by the COLA method [8]. One can tell the code to create either Gaussian or Non-Gaussian initial conditions. No potential is computed in the Gaussian case as opposed to the Non-Gaussian case, where the value is copied to a new variable, a data member of the particle. This is done in the file `2LPT.c` of the source code.

[1] https:/cullanhowlett.github.io/l-picola.

The greatest modifications regarding the computation of $\tilde{\phi}$ were made on `auxPM.c`, where the PM algorithm is implemented. The original steps starting from the particle's position are as follows:

1. CIC interpolation to the mesh to get the mass density $\tilde{\rho}_{i,j,k}$ at each mesh point.

2. FFT of $\tilde{\rho}_{i,j,k}$ and solving Eq. (2) in Fourier-space,

$$\mathbf{k}^2 \tilde{\phi}_{i,j,k}(\mathbf{k}) = \frac{3}{2} \frac{\Omega_{m,0}}{a} \tilde{\delta}_{i,j,k}(\mathbf{k}), \quad \mathbf{k} = (i,j,k)\,, \tag{5}$$

   where $\tilde{\delta}_{i,j,k}(\tilde{\mathbf{x}}) \equiv \tilde{\rho}_{i,j,k}(\tilde{\mathbf{x}}) - 1$.

3. Calculating the force at each mesh point,

$$\tilde{F}_{i,j,k}(\mathbf{k}) = \mathbf{k}\tilde{\phi}_{i,j,k}(\mathbf{k}), \tag{6}$$

   using the inverse FFT to get the force in real-space and the inverse CIC method to interpolate $\tilde{F}_{i,j,k}$ to particle's position.

In our modification we copied the result in step 2. to a new variable and performed a parallel FFT using the same C libraries (FFTW[2]) as in the original code. After that, we used the inverse CIC method to interpolate the potential to particle's position.

To output the potential at particle's position in ASCII format we simply added a new column in the output file just after the particle's position and velocity. For data in unformatted binary (i.e. `GADGET_STYLE` in L-PICOLA snapshot mode) the values are written as a compound block, which are associated with the particle positions through their output order. For the potential on the mesh we wrote a new function (under the preprocessor directive `GONGRID`) similar to that, which handles the output in snapshot mode. It writes the potential in a newly created data file (in the output folder) either in ASCII format or unformatted binary. The function is called at every output redshift.

In the next section we will show a snapshot simulation with the above mentioned modifications, i.e the gravitational potential at particle's position. The results are also representative for a test simulation of the potential on the mesh, as they merely differ in a CIC interpolation.

4 Test simulation

After we presented our modifications of L-PICOLA in the previous section, we want to show the results of a simulation outputting the potential at particle's position at redshift $z = 0$. We had run a simulation (with the COLA method enabled) from $z = 9$ to $z = 0$. The box has of edge length $L = 100\,h^{-1}\,\mathrm{Mpc}$ with $N_{sample} = 128$ particles and a mesh size $N_{mesh} = 128$ in one dimension. Further we set the matter density parameter $\Omega_{m,0} = 0.276$, the Hubble parameter $h = 0.7$, the power spectrum normalization $\sigma_8 = 0.83$ and primordial index to $n_s = 0.96$. Then, we plotted the potential with the HEALPix[3] hierarchical tessellation of the unit sphere [9].

[2] http://www.fftw.org/

[3] http://healpix.sourceforge.net

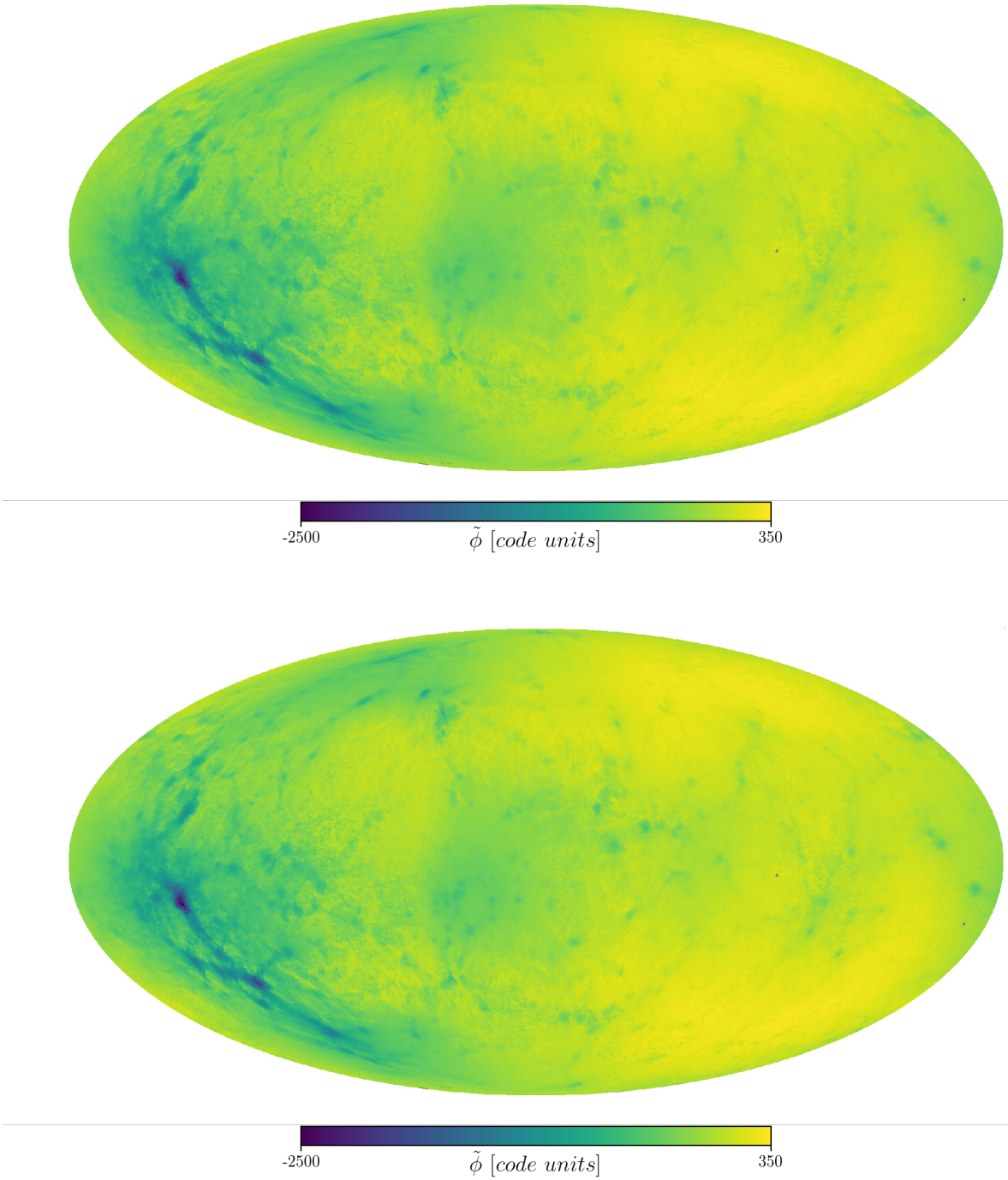

Figure 1: All-sky maps of the gravitational potential from data of L-PICOLA. *Top image:* Potential in code units obtained from the code output directly. *Bottom image:* Potential in code units obtained from particle's positions after solving eq. (7).

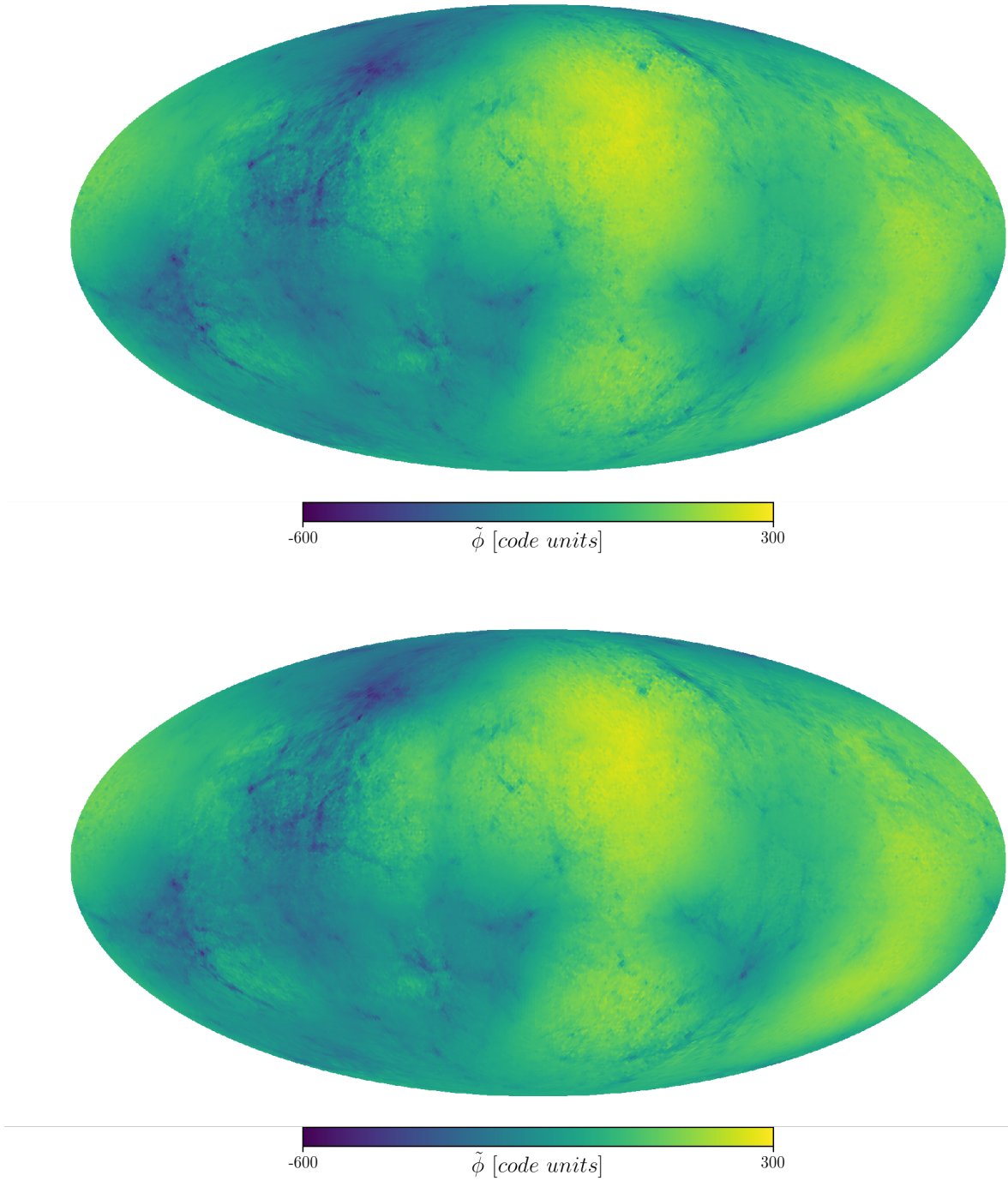

Figure 2: All-sky maps of the gravitational potential from data of GADGET-2. *Top image:* Potential in code units obtained from the code output directly. *Bottom image:* Potential in code units obtained from the mass density after solving eq. (7).

In the top image of Fig. 1 we show the gravitational potential in code units $\tilde{\phi}$ (see section 2 for details) of the L-PICOLA simulation up to an arbitrary constant. The map was first generated with a HEALPix pixelization parameter $N_{side} = 2^9$ - which corresponds to 3145728 pixels. This is enough to plot all $N^3_{sample} = 2097152$ data points. Then we used a HEALPy function `pixelfunc.ud_grade` to degrade the resolution to $N_{side} = 2^6$ - corresponding to 49152 pixels with a resolution ~ 54.98 arcmin. The blue color in the image represent regions of potential wells, i.e. regions of high mass density.

The bottom image of Fig. 1 shows the same simulation box. However, we used the particle's positions as input data for the pipeline to generate this plot. Besides the mapping procedure described in the last paragraph, this pipeline consist of the following steps:

1. We used the CIC method to interpolate the particle's positions to the mesh, thus getting the mass density $\tilde{\rho}_{i,j,k}$ $(i, j, k = 1, ..., N_{mesh})$.

2. We solved Eq. (2) in Fourier-space with a discretized Laplace operator, $\tilde{\nabla}^2\tilde{\phi}(\tilde{\mathbf{x}}) \simeq \tilde{\phi}_{i+1,j,k} + \tilde{\phi}_{i-1,j,k} + \tilde{\phi}_{i,j+1,k} + \tilde{\phi}_{i,j-1,k} + \tilde{\phi}_{i,j,k+1} + \tilde{\phi}_{i,j,k-1} - 6\tilde{\phi}_{i,j,k}$, yielding for the transformed potential,

$$\tilde{\phi}_{i,j,k}(\mathbf{k}) = \frac{3}{2}\frac{\Omega_{m,0}}{a}\frac{\tilde{\delta}_{i,j,k}(\mathbf{k})}{\omega^i + \omega^{-i} + \omega^j + \omega^{-j} + \omega^k + \omega^{-k} - 6}, \quad \omega \equiv e^{2\pi i/N_{mesh}}, \quad \mathbf{k} = (i, j, k)\,. \tag{7}$$

3. We transformed $\tilde{\phi}_{i,j,k}(\mathbf{k})$ back to real-space and used the inverse CIC interpolation to get the potential at particle's position.

The above pipeline was implemented in Python using the FFT libraries from NumPy. The transformations were performed with 128 equidistant sample points in each dimension and the full complex Fourier transform, which is appropriate for problems satisfying periodic boundary conditions. With this approach we want to prove that the potential computed with the modified L-PICOLA is consistent with the particle distribution. No difference can be found just by looking at the two maps. We will provide a more detailed analysis in the next section.

To check that we have not made an error in our calculations, we run the same simulation box using the same parameters and cosmological model with GADGET-2. Although the seed for the particle's positions was the same as in L-PICOLA, major differences in the algorithmic calculation of the particle interactions - splitting the potential into a long-range and short-range part - have not allowed us to compare them [1]. The results are shown in Fig. 2 using the same procedure as for L-PICOLA.

5 Analysis and verification

To compare the results presented in Fig. (1) and (2), we calculated the spherical harmonic power spectrum using the HEALPy function `sphtfunc.anafast` - the spectrum was taken from 49152 pixels corresponding to resolution ~ 54.98 arcmin. The results are plotted in Fig. (3). Except for the monopole, we see a less than 10 % discrepancy – relatively to *simulation* output – over all scales between the GADGET-2 outputs. We assume that the reason for the anomaly in the monopole could be the overall error ~ 0.44 in $\tilde{\phi}$ made by our poisson solver described in the previous section. The error was estimated from solving the poisson equation,

$$\nabla^2 f(x, y, z) = 2\left(2x^2 + 2y^2 + 2z^2 - 3\right) f(x, y, z), \quad f(x, y, z) \equiv e^{-\left(x^2+y^2+z^2\right)}, \tag{8}$$

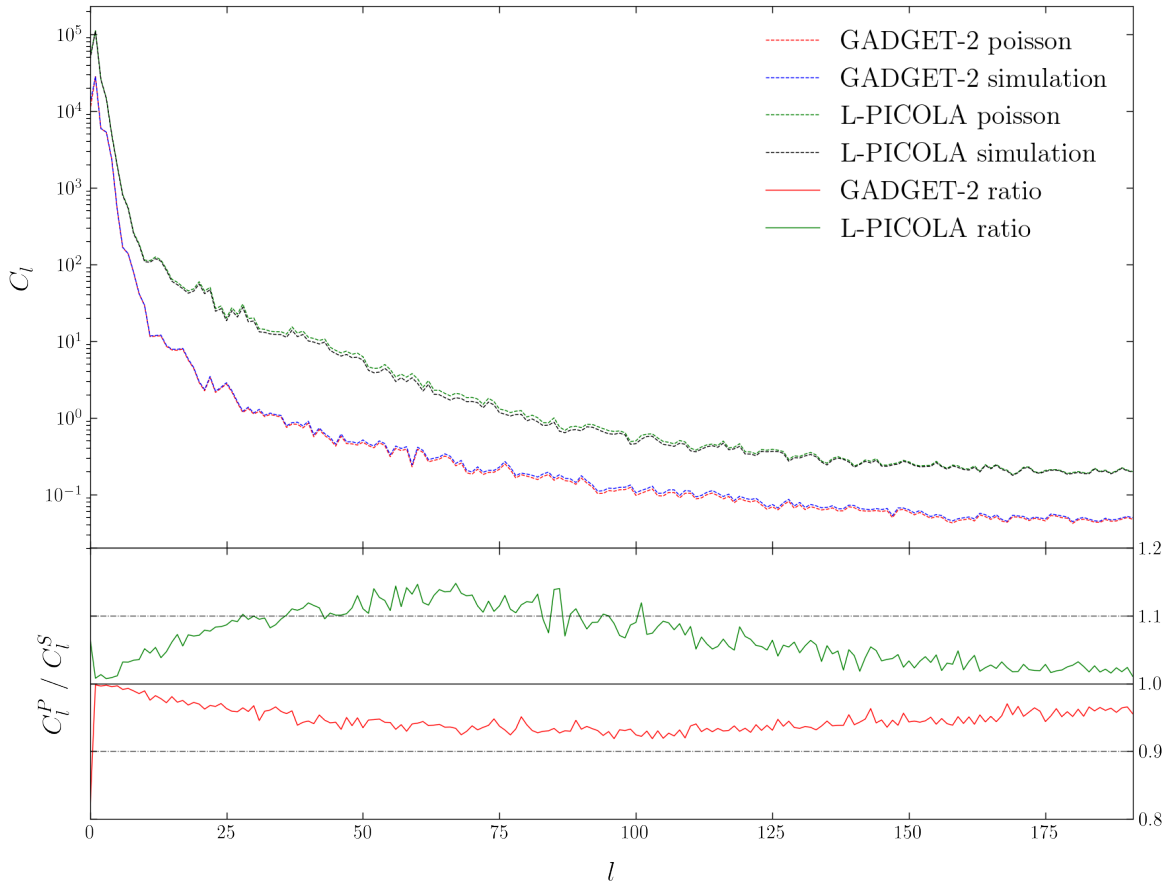

Figure 3: Spherical harmonic power spectrum of the gravitational potential from the HEALPix maps in Fig. 1 and 2 with an angular resolution ~ 54.98 arcmin. In the upper panel we compare the spectrum of $\tilde{\phi}$ from the simulation output at (*simulation*) to the result of Eq. (7) (*poisson*) for both L-PICOLA and GADGET-2. In the lower panel we took the ratio of *simulation* and *poisson*.

on an equidistant mesh with 128 samples in each dimension. For L-PICOLA we got similar results. However, due to higher gradients of the potential compared to GADGET-2, the spectra differ more than 10 % – relatively to *simulation* output – at scales $30 \lesssim l \lesssim 100$ and there is also an excess in the monopole.

The spectrum gives only a 2-dimensional analysis of the potential on the unit sphere. To investigate $\tilde{\phi}$ also in r-dimension, we divided the simulation box into 100 concentric shells around its centre, such that the outmost shell completely covers the box. We then took the average of $\tilde{\phi}$ in each shell and plotted it against the radius of the shell's mid-layer. These averages $\langle\tilde{\phi}\rangle_{shell}$ from the simulation output (*simulation*) and the calculated potential by the poisson solver (*poisson*) – as well as their ratio – are shown in Fig. 4 for both L-PICOLA and GADGET-2. In the lower panel we see, that the results from GADGET-2 agree within 5 % – relatively to *simulation* output – for all radii. The averages $\langle\tilde{\phi}\rangle_{shell}$ from L-PICOLA vary within 10 % – relatively to *simulation* output – for all radii. Comparing this plot with the

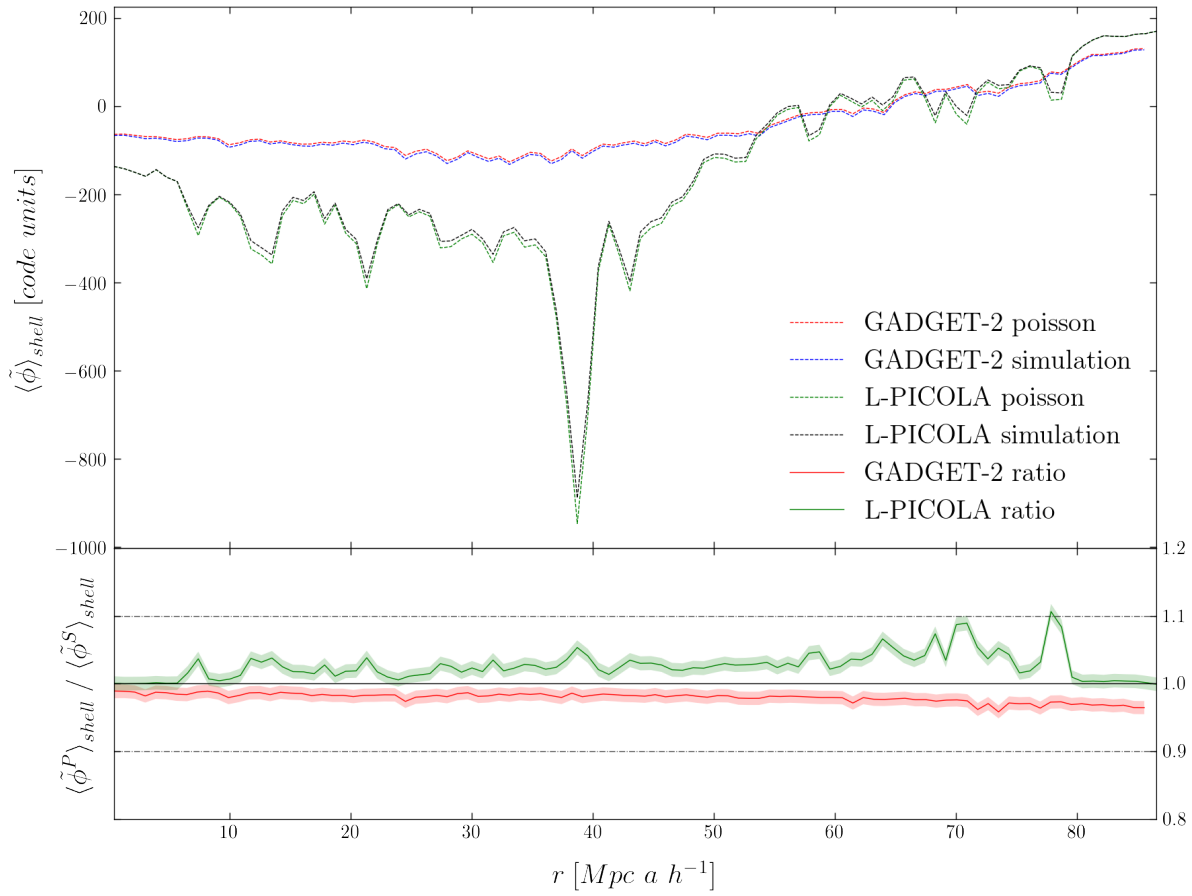

Figure 4: Gravitational potential averaged over concentric shells with the centre of the simulation box as the origin and a shell thickness $\sim 0.87\,\mathrm{Mpc\,a\,h^{-1}}$. In the upper panel we compare $\langle\tilde{\phi}\rangle_{shell}$ from the simulation output (*simulation*) to the result of Eq. (7) (*poisson*) for both L-PICOLA and GADGET-2. In the lower panel we took the ratio of *simulation* and *poisson*. The red and green area represent the largest error in solving Eq. (7) for GADGET-2 and L-PICOLA respectively.

one in Fig. 3, we noticed that the potential wells from the poisson solver are more distinctive than the wells from the simulation in case of L-PICOLA. The opposite is true for the results of GADGET-2. We are not sure what the cause of this tendency is, but we assume that the solver performs better on smooth scalar fields, as in the case of GADGET-2. To investigate this hypothesis we suggest trying to use more sample points for the FFT.

Furthermore, we compare the probability distribution function (PDF) of the potential from the simulation output (*simulation*) to the one from the poisson solver (*poisson*) for both codes. The results are shown in Fig. 5. The PDF's are plotted against 200 bins with size 19.25. We find that the $\tilde{\phi}$-values of the two outputs share a similar distribution for either simulation code. In Tab. 1 the sample means and standard deviations of $\tilde{\phi}$ of the two outputs and simulation codes are presented. The In the lower panel of Fig. 5 we compare the PDF's. The weighted average of their relative difference – relative to PDF($\tilde{\phi}^S$) – is less than 2.5 % and less than

5 %, while the difference of the means relatively to the RMS of their standard deviation is less than 2.9 % and less than 3.3 % for GADGET-2 and L-PICOLA respectively.

f	$\tilde{\phi}^{poisson}_{GADGET-2}$	$\tilde{\phi}^{simulation}_{GADGET-2}$	$\tilde{\phi}^{poisson}_{L-PICOLA}$	$\tilde{\phi}^{simulation}_{L-PICOLA}$
$\langle f \rangle$	-58.31	-63.30	-216.09	-203.91
σ_f	151.15	153.87	434.73	415.28

Table 1: Sample mean $\langle f \rangle$ and standard deviation σ_f of the gravitational potential for the various outputs and simulation codes.

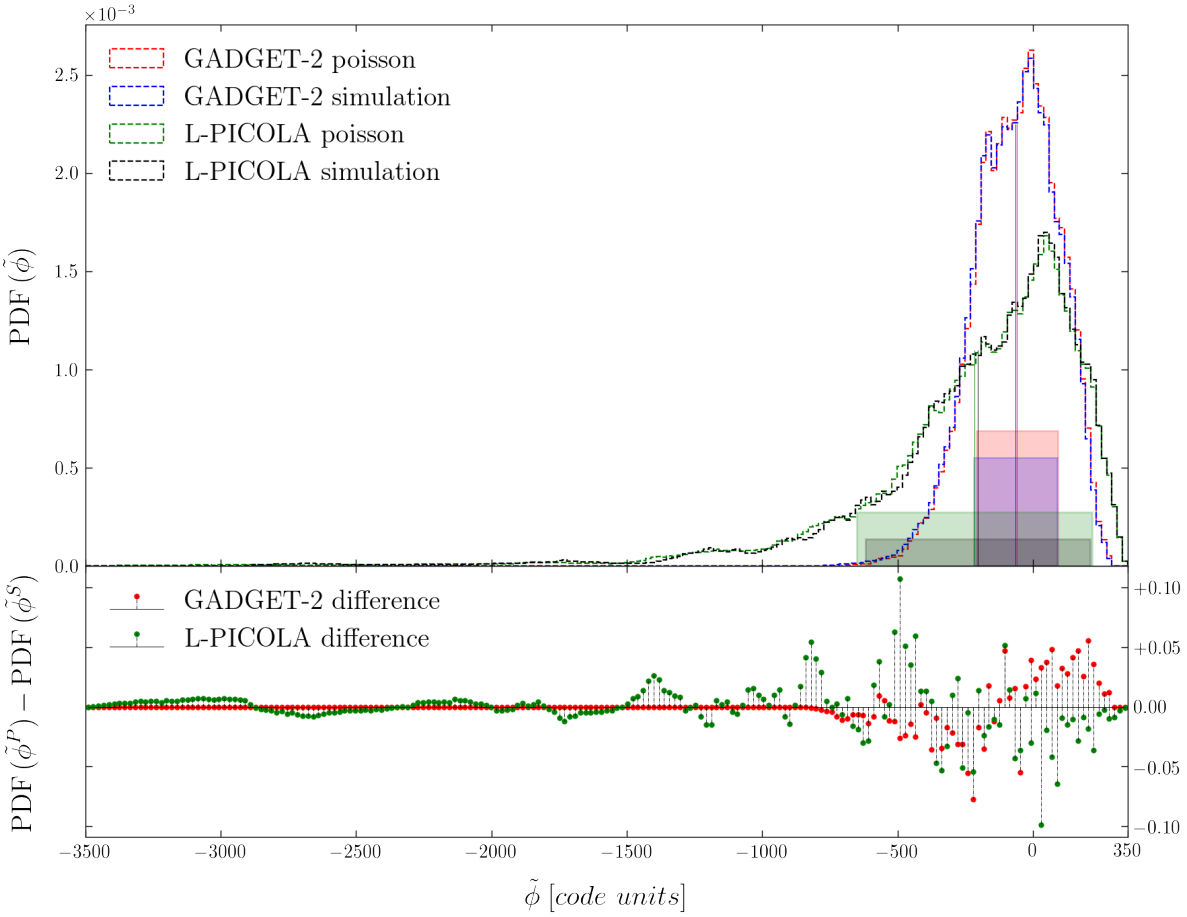

Figure 5: PDF of the gravitational potential. In the upper panel we compare the PDF ($\tilde{\phi}$) from the simulation output (*simulation*) to the result of Eq. (7) (*poisson*) for both L-PICOLA and GADGET-2. The solid vertical lines pinpoint the sample means of the gravitational potentials $\langle\tilde{\phi}\rangle$ and the half base-length of the colored rectangles the unbiased standard deviation $\sigma_{\tilde{\phi}}$ for the various outputs. In the lower panel the difference of the PDF's of the results is shown. The bin size is 19.25. The y-axis of both plots is scaled to 10^{-3}.

6 Conclusion

In this paper we introduced a modification of L-PICOLA to output the gravitational potential at particle's position and on an equidistant mesh. This could be useful for future constructions of all-sky lensing-potential and deflection-angle maps. Also, to help N-body simulations to directly simulate the CMB distortions caused by weak lensing much faster and thus provide enough simulation samples to increase the statistical significance of cosmological CMB surveys. We run this modified version on $\left(100\,h^{-1}\,\mathrm{Mpc\,a}\right)^3$ volume of space with 2097152 dark matter particles. The same simulation was also done using GADGET-2. We then looked at a single snapshot output at $z = 0$ to investigate the gravitational potential at particle's positions. This result than also induce the correctness of the potential on the mash, as they merely differ by a Cloud-in-Cell interpolation method. To prove that our modifications are correct, we solved the poisson equation of the potential using the mass overdensity field – particle's positions from the simulation output. The GADGET-2 simulation was used to show that we did not make any systematical error in the poisson solver implemented in Python. With the analysis of the spherical harmonic power spectrum from the HEALPix maps of the potential we found an agreement $C_{l,poisson}^{L-PICOLA}/C_{l,simulation}^{GADGET-2} < 10\,\%$ at scales $l \lesssim 30$ and $l \gtrsim 100$. The discrepancy around $\sim 15\,\%$ for $30 \lesssim l \lesssim 100$ are due to the small sampling of the FFT in the poisson solver and the bump of the monopole $l = 0$ are caused by an error of ~ 0.44 in the potential made by the solver as well. Furthermore, to complement the analysis in all 3 dimensions, we computed the average of the potential over concentric shells from the centre of the simulation box as a function its radius. The potential varied within $10\,\%$ relatively to the simulation output in all shells. Lastly, we took the 1-point distribution (PDF) of the potential. The difference of the means relatively to the RMS of their standard deviation is less than $2.9\,\%$ and less than $3.3\,\%$ for GADGET-2 and L-PICOLA respectively. The distributions show that the weighted average of the relative – relative to PDF($\tilde{\phi}^S$) – difference between the PDF of the simulation output and the PDF of calculated potential from the poisson solver is less than $2.5\,\%$ and less than $5\,\%$ for GADGET-2 and L-PICOLA respectively. Thus we conclude that our modified version of L-PICOLA is able to produce a gravitational potential field, as well as to sample the potential at the position of the particles. A further improvement of L-PICOLA would be to transfer our pipeline to generate a simulation with the potential in lightcone mode.

Acknowledgments

This research made use of MUSIC[4] [10], IPython, Jupyter notebook, NumPy, SciPy, Matplotlib, Healpy, Pynbody.

[4]To generate initial conditions for GADGET-2

References

[1] Springel V., *The Cosmological Simulation Code GADGET-2*, MNRAS **364** (2005) 1105-1134.

[2] Howlett C., Manera M. & Percival W.J., *L-PICOLA: A Parallel Code for Fast Dark Matter Simulation*, arXiv:1506.03737.

[3] Sgier R.J., Réfrégier A., Amara A. & Nicola A., *Fast Generation of Covariance Matrices for Weak Lensing*, arXiv:1801.05745v1

[4] Seo H.-J., Eisenstein D.J., ApJ **598** (2003) 720

[5] Kaiser N., MNRAS **227** (1987) 1

[6] Hockney R.W. & Eastwood J.W., *Computer Simulation using Particles*, (1988)

[7] Klypin A.A. & Holtzmann S.F., *Particle-Mesh Code for Cosmological Simulations*, arXiv:astro-ph/9712217.

[8] Tassev S., Zaldarriaga M. & Eisenstein D., *Solving Large Scale Structure in Ten Easy Steps with COLA*, JCAP **06** (2013) 036.

[9] Gorski K.M., *HEALPix: A Framework for High-Resolution Discretization and Fast Analysis of Data Distributed on the Sphere*, Astrophys. J. **622** (2005) 759.

[10] O. Hahn and T. Abel, *Multi-scale initial conditions for cosmological simulations*, MNRAS **415** (2011) 2101-2121